Ultraviolet Damage and Nucleosome Folding of the 5S Ribosomal RNA Gene†

Xiaoqi Liu,‡,§,|| David B. Mann,‡,§,⊥ Christine Suquet,‡ David L. Springer,▽ and Michael J. Smerdon*,‡

Biochemistry and Biophysics, School of Molecular Biosciences, Washington State University, Pullman, Washington 99164-4660, and Molecular Biosciences Department, Battelle Pacific Northwest National Laboratory, P7-56, Box 999, Richland, Washington 99352

Received July 29, 1999; Revised Manuscript Received October 27, 1999

ABSTRACT: The *Xenopus borealis* somatic 5S ribosomal RNA gene was used as a model system to determine the mutual effects of nucleosome folding and formation of ultraviolet (UV) photoproducts (primarily *cis*−*syn* cyclobutane pyrimidine dimers, or CPDs) in chromatin. We analyzed the preferred rotational and translational settings of 5S rDNA on the histone octamer surface after induction of up to 0.8 CPD/nucleosome core (2.5 kJ/m^2 UV dose). DNase I and hydroxyl radical footprints indicate that UV damage at these levels does not affect the average rotational setting of the 5S rDNA molecules. Moreover, a combination of nuclease trimming and restriction enzyme digestion indicates the preferred translational positions of the histone octamer are not affected by this level of UV damage. We also did not observe differences in the UV damage patterns of irradiated 5S rDNA before or after nucleosome formation, indicating there is little difference in the inhibition of nucleosome folding by specific CPD sites in the 5S rRNA gene. Conversely, nucleosome folding significantly restricts CPD formation at all sites in the three helical turns of the nontranscribed strand located in the dyad axis region of the nucleosome, where DNA is bound exclusively by the histone H3−H4 tetramer. Finally, modulation of the CPD distribution in a 14 nt long pyrimidine tract correlates with its rotational setting on the histone surface, when the strong sequence bias for CPD formation in this tract is minimized by normalization. These results help establish the mutual roles of histone binding and UV photoproducts on their formation in chromatin.

Ultraviolet (UV)[1] radiation forms several different photoproducts in DNA. The *cis*−*syn* cyclobutane pyrimidine dimer (CPD) is a classic example of a UV photolesion that is both mutagenic and carcinogenic in humans (*1*, *2*). The pyrimidine−pyrimidone (6−4) dimer [(6−4)PD] is the second most prevalent stable UV photoproduct in DNA and was also shown to play an important role in the mutation spectra of specific genes (*3*, *4*). These features may reflect the structural distortions in the DNA molecule induced at UV-damaged sites. For example, gel retardation and proton NMR experiments predict that CPDs cause a 7°−9° bend in the long axis of a double-strand DNA molecule (*5*, *6*).

In eukaryotic cells, DNA is packaged in a structural hierarchy called chromatin, beginning with the wrapping of DNA around core histone octamers (two each of histones H2A, H2B, H3, and H4) to form nucleosomes and ending with fully condensed chromosomes (reviewed in refs *7* and *8*). It is not surprising that this structural organization modulates both DNA damage formation and its subsequent repair (*9*). Indeed, in mixed sequence nucleosomes, the CPD distribution shows a striking 10.3 base (average) periodicity with a strong preference for the minor groove oriented away from the histone surface (*10*). Within the substructure of the nucleosome, this periodicity changes from an average of 10.5 bases over the central three turns of helix, containing the dyad axis of symmetry, to an average of 10.0 bases beyond this region (*11*; unpublished results). Furthermore, unfolding of nucleosome cores at very low ionic strengths dramatically changes the CPD distribution to a pattern similar to that of irradiated naked DNA even though the histones are tightly bound (*12*). Thus, DNA bending and/or flexibility plays a significant role in the modulation of CPD formation in nucleosomes (also see ref *13*).

Formation of nucleosomes onto UV-irradiated, mixed sequence DNA also results in an ∼10 bp repeat pattern of photoproducts (*14*), indicating that preexisting CPDs in DNA influence its rotational setting on the histone surface during nucleosome formation. Moreover, a strong modulation of CPD formation in nucleosomes was observed on a 134 bp yeast sequence (called HISAT), which contains a 40 bp polypyrimidine region with several long T-tracts (*15*). In this case, however, it was found that the CPD distribution in HISAT nucleosomes only partially resembles that of mixed sequence nucleosomes, since some of the enhanced CPD sites

† This study was supported by NIH Grant ES02614 from the National Institute of Environmental Health Sciences (to M.J.S.) and Department of Energy Contract DE-AC06-76RLO 1830 (to D.L.S.). D.B.M. was supported in part by a fellowship through Associated Universities Northwest, Inc., Northwest Division (AWU NW), under Grant DE-FG06-89ER-75522 or DE-FG06-92RL-12451 with the U.S. Department of Energy.

* Corresponding author: phone 509-335-6853; Fax: 509-335-9688; E-mail: smerdon@mail.wsu.edu.

‡ Washington State University.

§ These authors contributed equally to this work.

|| Present address: Department of Molecular and Cellular Biology, Harvard University, 16 Divinity Ave., Cambridge, MA 02138.

⊥ Present address: NMT-5, MS E506, Nuclear Materials Technology Division, Los Alamos National Laboratory, Los Alamos, NM 87545.

▽ Battelle Pacific Northwest National Laboratory.

[1] Abbreviations: CPD, *cis*−*syn* cyclobutane pyrimidine dimer; (6−4)PD, pyrimidine−pyrimidone (6−4) dimer; UV, ultraviolet; TS, transcribed strand; NTS, nontranscribed strand; T4 endo V, T4 endonuclease V; nt, nucleotide.

10.1021/bi991771m CCC: $19.00
Published on Web 12/29/1999

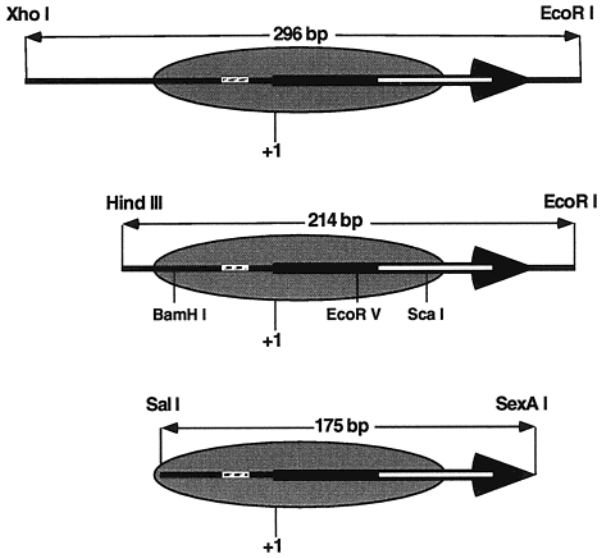

FIGURE 1: Schematic diagram of the three 5S rDNA fragments used in the study (296, 214, and 175 bp, top to bottom, respectively). The thick arrow designates the location of the 5S rRNA gene, and the shaded oval is the predominant nucleosome formation site (*18*). The 5S rDNA transcription initiation site is denoted by +1. The location of the 14 nt long pyrimidine tract is indicated by the hatched box, and the open box indicates the TFIIIA binding region. Restriction sites used to generate these fragments and map translational positions are also shown (middle diagram).

were close to the nucleosome surface (*15*). Thus, the correlation of CPD distributions with rotational setting in specific DNA sequences, particularly those that position the histone octamer, may vary considerably from the average distribution of CPDs in chromatin.

In this paper, the *Xenopus borealis* somatic 5S rRNA gene was used to examine the mutual effects of nucleosome folding and CPD formation. Since this gene forms well-positioned nucleosomes in vitro (*16*, *17*), we were able to examine (a) the effect of UV photoproducts on the orientation of 5S rDNA in the nucleosome and (b) the efficiency of CPD formation at specific sites within subdomains of a rotationally positioned nucleosome.

MATERIALS AND METHODS

Enzymes and Chemicals. The [γ-^{32}P]ATP (3000 Ci/mmol) used in this study was obtained from New England Nuclear (Boston, MA). *Eco*RI, *Hin*dIII, and *Xho*I were purchased from International Biotechnologies. T4 DNA polymerase was purchased from New England Biolabs (Beverly, MA), *Sex*AI and *Sal*I were purchased from Boehringer Mannheim Biochemicals (Indianapolis, IN). T4 endonuclease V (T4 endo V) was a generous gift from Dr. R. S. Lloyd (University of Texas Medical Branch, Galveston, TX).

5S rDNA Preparation. Three 5S rDNA fragments (*Eco*RI/*Xho*I, *Eco*RI/*Hin*dIII, and *Sex*AI/*Sal*I double digestion products of plasmid pKS-5S) with different lengths (296, 214, and 175 bp) were used in this study (Figure 1). Plasmid pKS-5S contains a single copy of the somatic 5S rRNA gene and was constructed as described previously (*18*). Briefly, after linearization of this plasmid with one restriction enzyme, DNA was dephosphorylated with calf intestinal alkaline phosphatase (Boehringer Mannheim) and labeled with [γ-^{32}P]-ATP by use of T4 polynucleotide kinase (U.S. Biochemical Corp.). A second restriction enzyme digestion produced a single end-labeled DNA fragment containing 120 bp of the 5S rRNA gene (see Figure 1). The resulting 5S rDNA fragments were recovered from a 2% agarose preparative gel, using a QIAEXII gel extraction kit (series 150), and dissolved in 10 mM Tris-HCl and 1 mM EDTA (TE buffer), pH 8.0.

Isolation of Nucleosome Core Particles. Nucleosome core particles, depleted of linker histones, were prepared from packed chicken erythrocytes (Lampire Biological Laboratories) as described by Libertini et al. (*19*).

Nucleosome Reconstitution. Reconstitution was achieved by histone octamer transfer as described previously (*18*). Briefly, 50 ng of end-labeled 5S rDNA was mixed with ~40 μg of chicken erythrocyte core particles (~20 μg of DNA) in 1 M NaCl, TE (pH 7.5), 0.2 mM phenylmethandsulfonyl fluoride (PMSF) for 30 min at 4 °C. The final concentrations of 5S rDNA and chicken erythrocyte core DNA in the reconstitution mixture were 0.6 ng/μL and 0.5 μg/μL, respectively. The samples were dialyzed against 0.6 M NaCl, TE (pH 7.5), and 0.2 mM PMSF for 12 h at 4 °C. A second 4-h dialysis step against 50 mM NaCl, TE (pH 7.5), and 0.2 mM PMSF completed the reconstitution. As a mock control, naked DNA was also mixed with core particles in TE (pH 7.5), and 0.2 mM PMSF without further stepwise dialysis.

Irradiation with UV Light. Both naked DNA and reconstituted nucleosomes were diluted with TE (pH 7.5) and 0.2 mM PMSF to a final DNA concentration of 50 ng/μL, irradiated under two low-pressure Hg lamps (Sylvania, model G30T8), providing predominantly 254-nm light at a flux of 4.3 W/m^2. UV flux was measured with a Spectroline DM-254N UV meter (Spectronics Corp., Westbury, NY).

Band Shift Assay. DNA band shift was used to examine the fraction of reconstituted 5S nucleosomes. The samples were run on 6% nondenaturing polyacrylamide gels in TBE buffer (89 mM Tris, 89 mM borate, and 2 mM EDTA, pH 8.3). Electrophoresis was run for 1.2 h at 120 V on a 8.3 × 10.2 cm gel.

DNase I Footprinting. DNase I digestions were carried out as described by Lutter (*20*). Briefly, reconstituted nucleosomes or DNA (0.1 mg/mL in 100 μL of 50 mM NaCl, TE, pH 7.5, and 0.2 mM PMSF) were incubated with 2.5 μL of DNase I (100 units/mL; Boehringer Mannheim, Indianapolis, IN) and 5 mM $MgCl_2$ as per manufacturer's instructions. Time points of 20 μL were taken at 0, 30, 60, and 120 s and added to 30 μL of 10 mM EDTA and 2% SDS. To remove the histones and other proteins, 6 μL of 5 mg/mL proteinase K (Boehringer Mannheim) was added and the mixture was incubated for 30 min at 37 °C. The samples were phenol-extracted, ethanol-precipitated, and run on a standard 6% sequencing gel.

Hydroxyl Radical Footprinting. Hydroxyl radical footprinting was carried out as described by Tullius et al. (*21*). Nucleosomes or DNA (with total DNA concentration of 0.1 mg/mL) were brought up in 50 mM NaCl and TE (pH 7.5) to a total volume of 170 μL. To this, 10 μL each of 20 mM sodium ascorbate, 0.6% H_2O_2, and Fe(II)−EDTA were added as separate beads to the side of the microcentrifuge tube. The reaction was started by mixing quickly with a micropipet or vortexing briefly. Time points (30 μL) were removed at 0, 30, 60, and 120 s and added to 5 μL of 0.1 M thiourea and 2 μL of 0.2 M EDTA to stop the reaction. After proteinase K digestion, the DNA samples were purified by

phenol extraction and ethanol precipitation and run on a 6% sequencing gel.

Translational Positioning Mapping. The translational position of the histone octamer on the 5S rDNA was assayed by a combination of micrococcal nuclease and restriction endonuclease digestion (*22*, *23*). Nucleosomes were reconstituted onto 214 bp unlabeled 5S rDNA (either UV-damaged or undamaged) as described above. To follow the reaction, a small amount (<0.01% by mass) of nick-translated 214 bp fragment was added to the 5S rDNA prior to reconstitution. A small aliquot of the samples was added to the digestion buffer (10 mM Tris-HCl, pH 7.5, and 0.5 mM $CaCl_2$) and digested with micrococcal nuclease at 37 °C for different times to determine the optimum time of digestion. After micrococcal nuclease digestion, the samples were deproteinized with proteinase K, concentrated by ethanol precipitation, and resuspended in TE. The DNA samples were then run on an 8% native polyacrylamide gel, and an autoradiograph was used to locate the ~147 bp band, which was recovered for subsequent experiments. Following cleanup and quantification of the DNA, the ~147 bp core DNA samples were cleaved with either *Bam*HI, *Eco*RV, or *Sca* I. The samples were dephosphorylated with calf intestinal phosphatase, end-labeled with T4 polynucleotide kinase, and run on an 8% denaturing polyacrylamide gel for 4 h at 40 W constant power.

Digestion with T4 DNA Polymerase. T4 DNA polymerase digestion was carried out as described by Gale et al. (*10*), taking advantage of the 3′ → 5′ exonuclease activity of T4 DNA polymerase in the absence of deoxynucleotide triphosphates. Briefly, after heat denaturation in boiling water for 10 min, DNA samples were dissolved in T4 DNA polymerase digestion buffer (33 mM Tris−acetate, pH 7.9, 66 mM potassium acetate, 10 mM magnesium acetate, 10 mM dithiothreitol, and 1 mg/mL BSA) and incubated with 6 units of enzyme. The reaction was incubated at 37 °C for 2 h to ensure the completion of the reaction and halted by incubation at 65 °C for 10 min.

Mapping and Quantitation of CPDs with T4 Endo V. Prior to T4 endo V digestion, DNA was phenol-extracted, ethanol-precipitated, and resuspended in T4 endo V buffer [20 mM Tris-HCl (pH 7.4), 10 mM EDTA (pH 8.0), 100 mM NaCl, and 100 μg/mL BSA]. T4 endo V [1 μL of a 200-fold dilution of enzyme stock (~400 ng/μL)] was then added and the reaction was incubated at 37 °C for 30 min. After addition of gel loading buffer to stop the reaction, the samples were heat-denatured and run on 8% polyacrylamide/8 M urea sequencing gels for 2.5 h at 1600 V (*24*). The gels were then vacuum-dried and exposed to phosphorimager screens (Molecular Dynamics). To quantify bands on gels for DNA damage formation, ImageQuant (Molecular Dynamics) and PeakFit 4.0 (SPSS, Inc) software were used. A straight-lined scan of the gel profile, covering the central $^3/_4$ of a lane, was obtained by the ImageQuant software. The data were then subjected to peak deconvolution analysis with the PeakFit software, using a basis spectrum line shape of Gaussian plus Lorentzian curves (for more details see ref *25*). The sum of all CPD-corresponding bands and the band representing the whole-length fragment was defined as 100%.

RESULTS

Effect of UV Photoproducts on the Rotational Setting of 5S Nucleosomes. Three different DNA fragments containing the 5S rRNA gene were used in this study (Figure 1). The shaded oval shows the most frequent (or preferred) position of the histone octamer relative to the various elements of the 5S rRNA gene. The longer fragments (214 and 296 bp) were used in these studies to allow more rotational and translational freedom for the 5S rDNA on the histone surface than the shortest fragment (175 bp). (For a discussion of rotational and translational setting, see ref *9*). We expected that changes induced by UV photoproducts may be more apparent with these longer fragments. On the other hand, the short fragment facilitates measurement of the exact positions of CPD modulation in the 5S nucleosome by constraining the rotational and translational settings (see below). After in vitro reconstitution with these fragments (see Materials and Methods), DNA band shift analysis, as done previously in our laboratory (e.g., see ref *18*), was used to monitor the formation of nucleosomes with both irradiated and unirradiated 5S rDNA fragments. In agreement with our previous competitive reconstitution experiments (*18*), UV irradiation decreases nucleosome formation on 5S rDNA (data not shown). As the levels of (6−4)PDs at specific sites can be appreciable at higher UV doses (*1*, *2*), it is likely that these lesions are responsible for much of this inhibition.

To analyze the effect of UV photoproducts on 5S rDNA positioning in nucleosomes, the rotational setting of 5S rDNA molecules was analyzed by both DNase I and hydroxyl radical footprinting (Figure 2). In nucleosomal DNA, DNase I cuts where the minor groove faces away from the histone surface, giving an ~10 base repeat pattern on denaturing gels (reviewed in ref *20*). However, because of its modest sequence specificity, the relative intensities of the bands produced in a digestion of a given sequence will vary considerably (e.g., Figure 2A, lanes 10−17). Reconstitutions were performed following different UV doses (from 500 J/m^2 to 2.5 kJ/m^2) yielding 0.6−0.8 CPD/nucleosome core DNA (147 bp). An example is shown in Figure 2A, where the strong cut sites (indicated by stars) are separated by multiples of ~10 bases (compare the "reconstitute" lanes to the DNA lanes; from top to bottom the positions are −65, −34, −5, 47, 59, and 78 with respect to the transcription start site of the 5S gene). A comparison of the undamaged reconstitutes (Figure 2A, lanes 1−4) to UV-damaged reconstitutes (Figure 2A, lanes 5−8) reveals that there are no significant differences in the digestion of the damaged and undamaged samples. This was the case for all UV doses tested.

Hydroxyl radical footprinting measures the accessibility of the minor groove and DNA phosphate backbone to the solvent (*21*). In nucleosomal DNA, this translates to a periodic banding pattern reflecting the ~10 bp repeat of the DNA molecule as it wraps around the histone octamer (*16*). Analogous to the DNase I footprint, the hydroxyl radical footprint does not show any clear differences between the undamaged and UV-damaged samples (Figure 2B). This could be due to the damage causing only a local distortion in the DNA structure that is not propagated along the DNA. Such propagation may be blocked by the strong positioning elements of the 5S sequence. Alternatively, the mixture of UV-damaged fragments, of which only ~20% of the bases

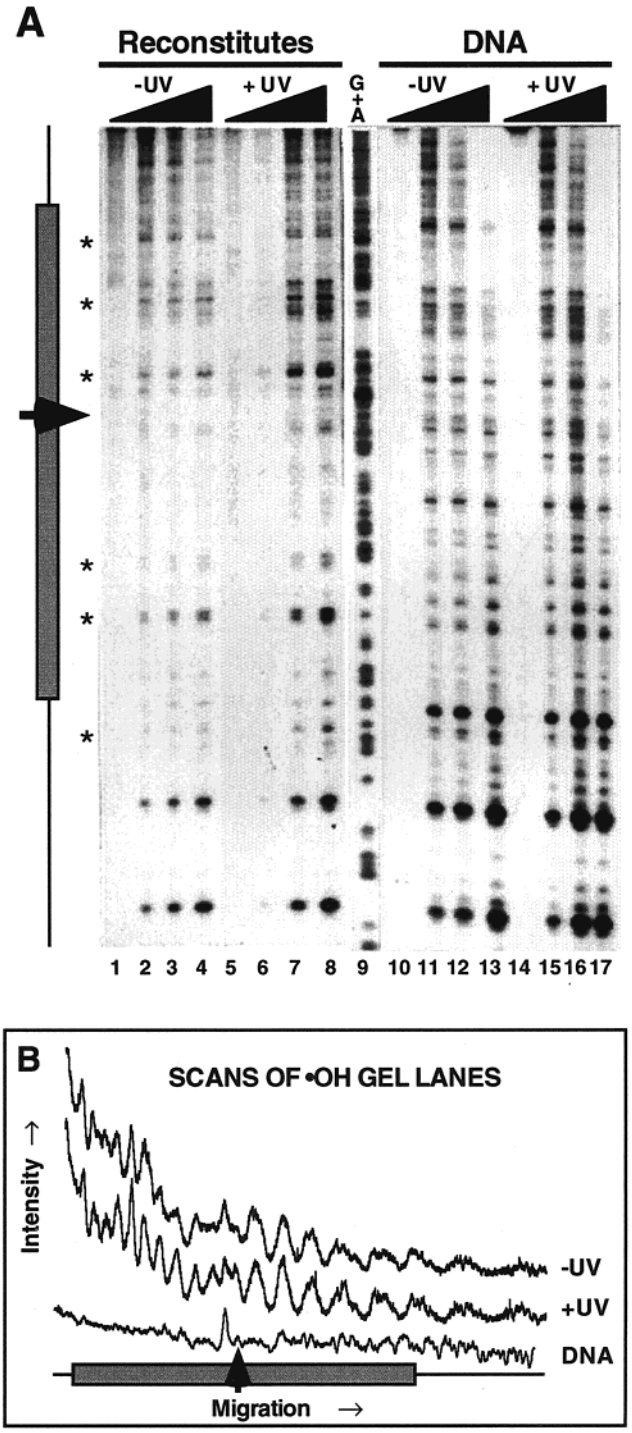

FIGURE 2: Rotational positioning of the 5S rDNA fragment in nucleosomes is not changed by UV irradiation. (A) Time course of DNase I digestions of reconstituted and naked 296 bp 5S rDNA fragment. Digestion times of 0, 30, 60, and 120 s were used in each reaction set. Lanes 1−4, undamaged reconstitutes; lanes 5−8, 500 J/m^2 UV-damaged reconstitutes; lanes 10−13, undamaged DNA; lanes 14−17, 500 J/m^2 UV-damaged DNA. Lane 9, marked G + A, is a dideoxy guanine plus adenine sequence reaction of the 296 bp 5S rDNA fragment. Stars to the left of the figure indicate the locations of strong DNase I cut sites and are located at (from top to bottom) −65, −34, −5, 47, 59, and 78 with respect to the transcription start site of the 5S rRNA gene. (B) Scans of hydroxyl radical reactions with UV-damaged (500 J/m^2) and undamaged reconstituted samples. The shaded box in each figure indicates the principal location of the positioned nucleosome, while the arrow indicates the location of the dyad axis.

are damaged at the most frequently damaged sites, may not give a large enough signal to see subtle changes. However, it is clear that the rotational setting of the 5S rDNA fragments is not markedly changed by simple formation of UV photoproducts at any site within these fragments.

Effect of UV Photoproducts on the Translational Setting of 5S Nucleosomes. To map the translational positions of reconstituted 5S nucleosomes, micrococcal nuclease digestion was coupled with restriction endonuclease digestion (*23*; also see Materials and Methods). Three different restriction enzymes, *Bam*HI, *Eco*RV, and *Sca* I, were chosen to give cuts near the 5′ edge, middle, and 3′ edge (Figure 3) of the most prevalent translational setting of the histone octamer observed for larger fragments (i.e., with a dyad near +10). Comparisons of the restriction digests of UV-damaged and undamaged samples indicate that UV irradiation does not disrupt the DNA sufficiently to cause measurable changes in the translational positions (e.g., compare band patterns of the *Sca*I and *Eco*RV digests for damaged and undamaged samples in Figure 3 panels A and B). Furthermore, the multiple bands obtained after restriction enzyme digestion indicated that several different translational settings are possible for the 214 bp fragment (e.g., see Figure 3B). Quantitation of gel patterns for both the UV-irradiated and unirradiated 214 bp fragments indicate that (a) about 40% of the nucleosomes are positioned at (or close to) prominent locations reported previously for larger fragments containing the somatic 5S rRNA gene (i.e., dyad near the transcription start; see refs *16* and *17*); (b) about 27% of the nucleosomes were positioned at the 3′ end of the 214 bp fragment (dyad at about +58); and (c) about 20% of the nucleosomes were located at the 5′ end (dyad at about −9) (Figure 3C). Several minor positions were also observed (Figure 3C) and UV irradiation did not change the relative proportion or lengths of the associated bands. The high proportion of nucleosomes positioned at the ends of these fragments presumably reflects the inherent preference of histone octamers for DNA ends (*26*).

UV Damage Distribution in Nucleosomal DNA. In view of the results with competitive reconstitutions (*18*), showing a general inhibition of nucleosome formation with UV-damaged 5S rDNA, we wished to determine if there are specific damage sites that play a major role in inhibiting (or facilitating) nucleosome formation. Therefore, we isolated both the free DNA and nucleosomal fractions of a reconstitution onto damaged or undamaged 5S rDNA and performed a T4 DNA polymerase−exonuclease digestion on them to map the locations of the DNA damage in each (Figure 4). T4 DNA polymerase has a 3′ → 5′ exonuclease activity in the absence of deoxynucleotide triphosphates (*27*), and this exonuclease activity is quantitatively blocked by both CPDs and (6−4)PDs (*28*). A baseline map of the relative damage levels at specific sites within the transcribed strand (Figure 4C) indicates that many of the most heavily damaged sites are predicted to be close to the histone surface with a high likelihood of impacting nucleosome formation and or positioning. However, the results of the T4 pol−exo digestion indicate there are no marked differences in the damage profiles of the nucleosomal and free DNA fractions of a reconstitution reaction (Figure 4B, compare D to N lanes). Thus, there appears to be little (or no) difference between specific UV photoproduct sites in the 5S rDNA gene that either obstruct (or support) nucleosome folding.

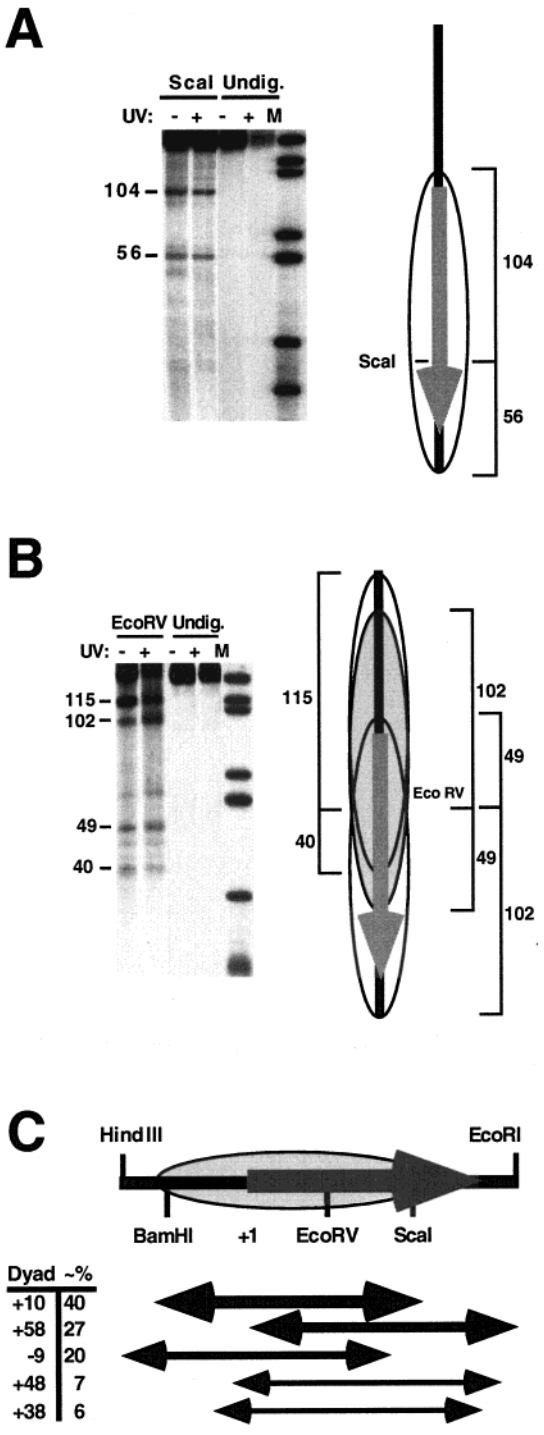

FIGURE 3: Translational positioning of 5S rDNA fragment in nucleosomes is not changed by UV irradiation. (Panels A and B) Polyacrylamide gels (6%) of the 214 bp 5S rDNA fragments following nucleosome reconstitution, digestion with micrococcal nuclease, DNA isolation, ^{32}P end-labeling, and digestion with either *Sca*I (A) or *Eco*RV (B). Fragments were either irradiated (+) or not (−) with 2500 J/m^2 UV irradiation prior to nucleosome reconstitution. Control lanes are undigested samples and molecular size markers (M). The dark band at the top of each lane (140−150 bp) is DNA from the chicken erythrocyte core particles, which are present during the end-labeling reaction. (C) Schematic summary of relative frequency of nucleosome positions when digested by micrococcal nuclease at 37 °C. Pairs of fragments totaling 150−160 bp were used for determining lengths from restriction cut sites to nucleosome edges following the moderate micrococcal nuclease digestion. The thickness of the lines indicates the relative fraction of nucleosomes at a given position.

Modulation of CPD Formation by Nucleosome Folding. CPD formation in naked 5S rDNA and nucleosomes was examined after different UV doses, using the 175 bp fragment. Purified DNA was extracted from these samples and incubated with T4 endo V, which makes single-strand cuts specifically at CPD sites (*29*). After electrophoresis on DNA sequencing gels, the gels were exposed to phosphorimager screens and quantified by peak deconvolution (see Materials and Methods). The average CPD formation in each strand was calculated from the percentage of full-length, uncut 175 base band (e.g., see dark bands in lanes 1−8 of Figure 6A), assuming a Poisson distribution of CPD formation per DNA molecule (*30*). Figure 5 shows the comparison of total CPD formation in naked DNA (dashed line) and reconstituted nucleosomes (solid line) for each strand at different UV doses. Clearly, nucleosome folding has little effect on total CPD formation in either strand, although there is an ∼5-fold difference in yield of CPDs between the two strands (Figure 5). Interestingly, this strand difference is only partly accounted for by the dipyrimidine difference in these strands (*31*) and must reflect other features of the fragment.

The bands produced by T4 endo V cleavage allows comparison of individual CPD sites between naked DNA and nucleosomes. Nucleosome folding has little effect on CPD formation at any of the CPD sites in the transcribed strand (data not shown; although see Figure 6C). However, inhibition of CPD formation was evident at some sites in the dyad axis region of the nontranscribed strand (Figure 6A, stars). A total of 18 CPD sites in the transcribed strand (TS), and 16 CPD sites in the nontranscribed strand (NTS) were analyzed quantitatively by calculating the percentage of total intensity in each lane at each CPD site for varying UV doses. An example for CPD formation at the 5′-TCC-(+4) site in the NTS (see Figure 6A, arrow), is shown in Figure 6B. Linear regression yields two slopes (K_D for naked DNA and K_N for nucleosomes) and, in the case of 5′-TCC-(+4), the yield of CPDs is 2.3-fold higher in naked 5S rDNA. These slopes were determined for each CPD site, and their ratios are plotted in Figure 6C. In these plots, a K_N/K_D value < 1.0 corresponds to an inhibition of CPD formation by nucleosome folding, while values close to 1.0 indicate little (or no) difference. As shown in Figure 6C, nucleosome formation has little effect on CPD formation at most sites in the transcribed strand, with the possible enhancement of CPD yield at two sites near the extreme edge of the nucleosome (near +80). On the other hand, significant inhibition was detected at several sites in the nontranscribed strand, located in the ∼30 bp dyad region of the nucleosome (hatched box in Figure 6 panels A and C). [The averages and variations (±SE) of K_N/K_D within different nucleosome subdomains are shown by the midpoints and widths of the shaded rectangles.]

From our results with mixed sequence nucleosomes (*10*), we anticipated that CPD formation would be reduced at sites where the minor groove faces toward the histone surface and enhanced at sites where the minor groove faces away from the histone surface. To address this possibility, a 14 nt long pyrimidine tract in the transcribed strand was analyzed in more detail (Figure 7A), since it spans over one complete turn of the 5S rDNA helix. This tract is 121−135 bases from the 5′ end of the TS of 5S rDNA, or 22−36 bases 5′ of the prominant nucleosome dyad (see Figure 1). Resolution of

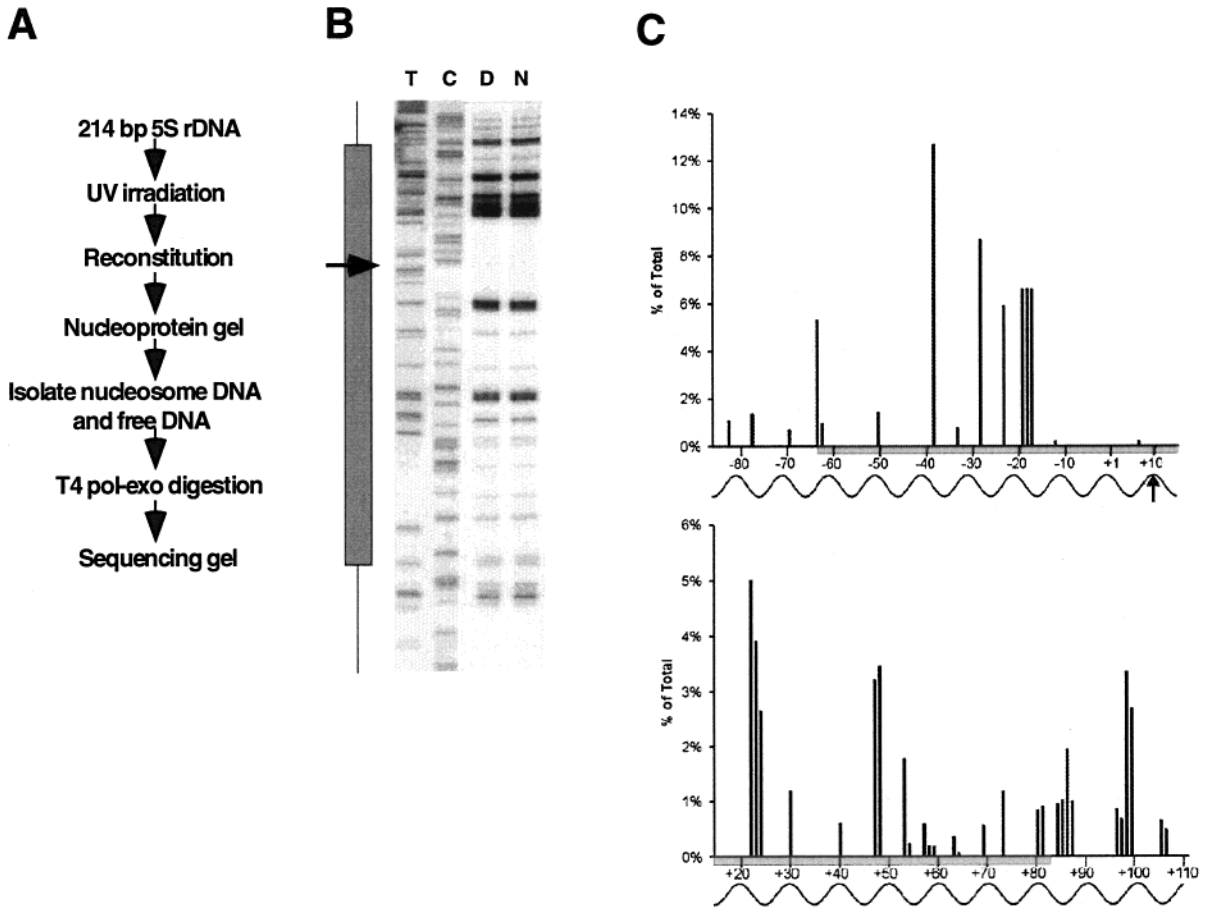

FIGURE 4: Mapping of UV photoproduct distribution in the transcribed strand of nucleosomal and free DNA fractions of reconstitutes. (A) Flow diagram for CPD mapping experiments on nucleosomal and free DNA in reconstituted samples. (B) The 214 bp 5S rDNA fragment was UV-irradiated with 500 J/m^2 (resulting in 0.8 CPD/214 bp fragment), reconstituted onto nucleosomes. Nucleosomal (N) and free DNA (D) fractions of reconstitutes (present in approximately equal amounts) were isolated from a 0.7% agarose gel and digested with T4 DNA polymerase−exonuclease. The digestion products were run on an 8% sequencing gel to map the total UV photoproduct distribution. Lanes marked T and C are dideoxy sequencing lanes of the 5S rDNA fragment. The shaded box and arrow are as described in Figure 2. (C) UV damage levels at different sites in the transcribed strand and their relationship to the histone surface. Bars denote the percentage of total signal over the entire strand. The three equal bars at −17 to −20 are one-third of the total signal for a broad band at the run of four Ts at this position that could not be resolved by deconvolution. Numbers at the bottom of each panel are the base locations with respect to the start site of the 5S gene. Sinusoidal lines indicate the approximate path of the DNA strand along the histone surface, as determined by hydroxyl radical footprinting (Figure 2; see ref *16*), where the top of the curve denotes locations furthest away from the histone surface. The thick, shaded bar denotes the position of the predominant nucleosome position with the dyad at about +10 (arrow).

the 13 CPD-forming sites (bands) in this sequence required a much longer gel running time (~6 h, see Figure 7B), where most of the shorter DNA fragments run out of the gel. Therefore, the percent intensity for just the 13-band cluster was used (rather than the percent of total intensity in a lane) to compare the CPD distribution along the histone surface (Figure 7C). A marked sequence influence on CPD formation is observed in this tract, with a strong bias in CPD formation near the 5′ end (Figure 7B,C). To minimize this influence on the CPD pattern, the ratio between the two percentages at each CPD site (i.e., R_N/R_D) was plotted against location in the 5S rDNA (Figure 7D). As can be seen, a correlation is now observed between CPD formation and the rotational setting. For example, the lowest value of R_N/R_D (i.e., the strongest inhibition of CPD formation by nucleosome folding) is detected at site CC(−19), the site closest to the histone surface (open triangle in Figure 7 panels A and D). In contrast, high values of R_N/R_D were observed at site CC(−24) and TC(−14) (stars in Figure 7 panels A and D), which are both strong DNase I and hydroxyl radical cleavage sites. Thus, nucleosome formation causes modulation of CPDs in the pyrimidine tract of 5S rDNA, and this modulation corresponds to the rotational setting of 5S rDNA on the histone surface.

DISCUSSION

Considering the fact that UV photoproducts can induce local distortions in DNA (*2*), it is conceivable that they may affect nucleosome stability, rotational positioning, and translational positioning. By use of a DNA supercoil assay to estimate nucleosome density, it was shown that only about half the number of nucleosomes can be reconstituted onto circular plasmid DNA following 3000 J/m^2 UV irradiation, where almost 3 photoproducts/nucleosome were formed (*32*). Furthermore, using *Escherichia coli* and *Drosophila* photolyases to specifically remove CPDs and (6−4)PDs, respectively, these authors were able to distinguish the effects of the two different photoproducts. When damaged DNA carrying mainly CPDs was used as a substrate for reconstitution, nucleosome formation was about 95%. In contrast, damaged DNA carrying mainly (6−4)PDs was virtually unable to supercoil around histone octamers to form nucleo-

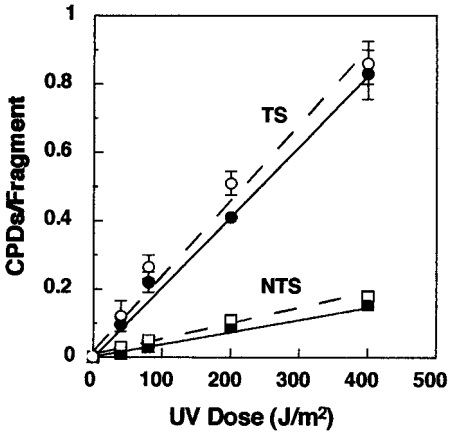

FIGURE 5: UV dose−response of the overall CPD formation in 5S rDNA. The 175 bp 5S rDNA fragment was end-labeled on the transcribed strand (TS) or the nontranscribed strand (NTS). After naked DNA (○, □) or reconstituted nucleosomes (●, ■) were irradiated with different UV doses, DNA was purified, digested with T4 endo V, and run on a sequencing gel. Total CPD formation was calculated assuming a Poisson distribution ($-\ln P_0$), where P_0 is the fraction of DNA resistant to T4 endo V digestion (*30*). Data represent the average of three independent experiments (mean ± 1 SD).

somes (*33*). This suggests that regions carrying (6−4)PDs tend to retain a nucleosome-free conformation. The inhibition effect of UV photodamage to DNA on nucleosome formation was also observed in *Xenopus borealis* 5S rDNA (*18*). Competitive reconstitution analysis showed a 1.5-fold decrease of core histone binding to the 214 bp 5S rDNA fragment following irradiation with 2.5 kJ/m^2, compared with undamaged DNA. Interestingly, nucleosome formation was *enhanced* when 5S rDNA was damaged with benzo[*a*]pyrene diol epoxide (BPDE), implying that the type of DNA lesion is important in determining how DNA damage will affect nucleosome folding (*18*).

The effect of DNA damage on nucleosome positioning is another important consideration. When nucleosomes are reconstituted onto UV-damaged mixed sequence DNA, they favor a rotational setting that places the lesions away from the histone surface (*14*). Furthermore, these nucleosomes tend to adopt a translational setting that excludes photoproducts from the central dyad region (*14*). In addition, the 134 bp HISAT sequence, with a defined rotational setting, was used to investigate the influence of UV photoproducts on nucleosome positioning. Although CPD formation in preformed nucleosomes had no effect on the rotational setting of HISAT DNA, when this DNA was extracted and reconstituted again into nucleosomes, the rotational setting was clearly changed (*15*).

In the present study, we examined the effect of UV damage on longer DNA fragments (than the HISAT DNA) containing the nucleosome positioning 5S rRNA gene where the translational and rotational flexibility is (presumably) greater than in a 134 bp fragment. However, in agreement with Schieferstein and Thoma (*15*), neither DNase I nor hydroxyl radical footprinting showed any significant changes in the patterns of digestion between the undamaged and UV-damaged samples (Figure 2B). This indicates that CPDs do not significantly alter the rotational setting of 5S rDNA in the nucleosome although, at many sites, the damage is expected to be located close to the histone surface. One

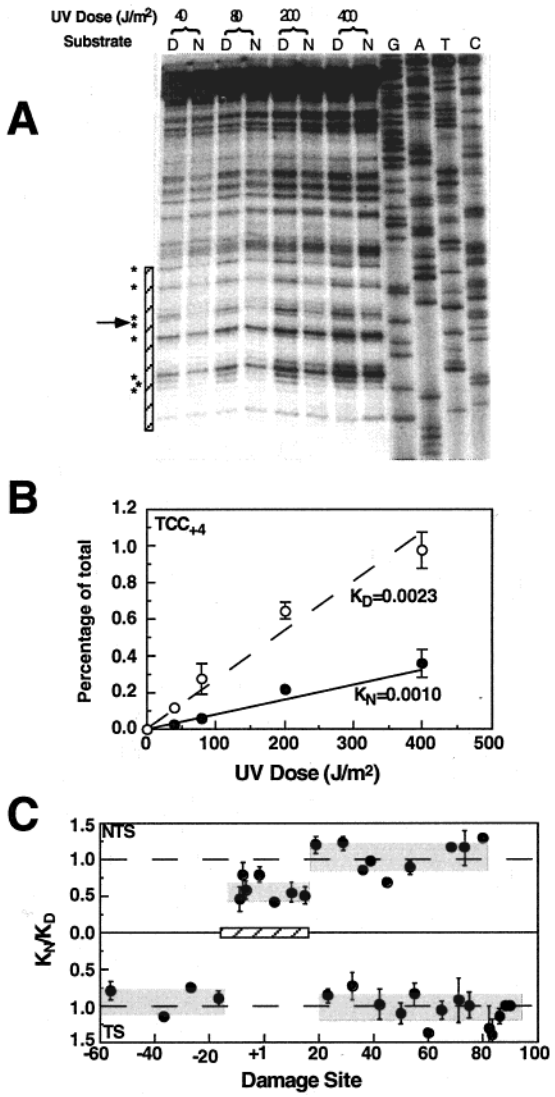

FIGURE 6: Modulation of CPD formation by nucleosome folding in 5S rDNA. (A) Representative phosphorimage of CPD distribution in the 5S rDNA sequence when the NTS is labeled. Naked 5S rDNA (D) or 5S nucleosomes (N) were irradiated with different UV doses, and the DNA was purified, treated with T4 endo V, and run on a DNA sequencing gel. The right four lanes are Sequenase reaction lanes. Stars on the left indicate sites where CPD formation is inhibited by nucleosome folding, and the hatched bar shows the location of the central (dyad) region of the 5S rDNA nucleosome. (B) Quantitation of CPD formation at site 5′-TC(+4)C (designated TCC_{+4}; arrow in panel A) for naked DNA (○) and nucleosomes (●). Data represent the mean ± 1 SD (three separate experiments) of the percentage of total intensity in a lane at site TCC_{+4} for four different UV doses. Lines represent linear regressions of the data with the corresponding slopes K_D (free DNA) and K_N (nucleosomes). (C) The 5S rDNA fragment was irradiated either as naked DNA or as reconstituted nucleosomes. As shown in panel B, the percentage of total intensity in a lane was determined at each CPD site for four different UV doses, and the slope of each curve was obtained after linear regression of the data. The ratio of the two slopes (K_N/K_D) is plotted at each CPD location in the sequence, and each data point represents the mean ± 1 SD for three separate experiments. A value of $K_N/K_D < 1.0$ indicates nucleosome folding inhibits CPD formation, while the dashed lines correspond to the values of K_N/K_D equal to 1.0 (no difference in CPD yield). Numbers on the abscissa are in base pairs from the 5S rRNA gene transcription initiation site (+1). The 30 bp dyad region of the 5S nucleosome is indicated by the hatched bar. The averages and variations (± SE) of the different nucleosome subdomains are represented by the midpoint and width, respectively, of the four shaded rectangles.

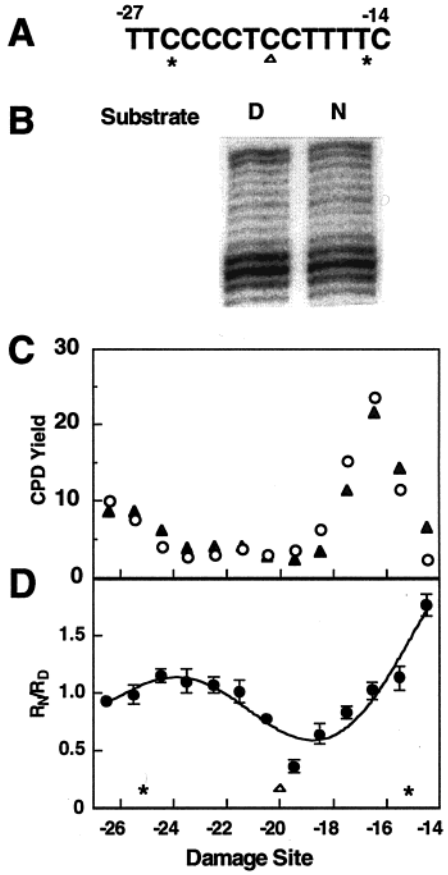

FIGURE 7: Correlation between DNA damage formation and rotational setting in the 14 nt long pyrimidine tract. (A) Sequence of the 14 nt pyrimidine tract in the 175 bp *Sex*AI−*Sal*I 5S rDNA fragment. Stars represent sites farthest away from the histone surface (strong DNase I and hydroxyl radical cleavage sites), and the triangle denotes the site closest to histone surface. Numbers above the sequence denote nucleotides from the transcription initiation site of the 5S rRNA gene. (B) Representative gel showing CPD formation in the pyrimidine tract. Either naked DNA (D) or reconstituted nucleosomes (N) were irradiated with 400 J/m^2. After DNA purification, the samples were cut with T4 endo V and run on a DNA sequencing gel long enough to resolve the 13 target bands. (C) Percentage of total intensity of each band (CPD yield) within the pyrimidine tract is shown for naked DNA (○) and reconstituted nucleosomes (▲). (D) Ratio of the two percentages (R_N/R_D) shown in panel C is plotted at each CPD site in the 5S rDNA fragment. Data represent mean ± 1 SD of seven separate experiments. Stars and triangle are the same as in panel A.

explanation for this result is that UV damage may cause only local distortions in nucleosome structure, which are not propagated along the DNA for any great length. These distortions could potentially be constrained by the strength of the nucleosome positioning element as observed with HMG(I)Y binding (*34*). Alternatively, the nucleosome may shift translationally by an integral number of helical repeats to position the damage in a more energetically favorable location. To address the later possibility, micrococcal nuclease-coupled restriction endonuclease analysis (*23*) was performed to detect the translational positions of undamaged and UV-damaged 5S nucleosomes (Figure 3). Once again, no significant changes in the translational positions between damaged and undamaged samples were found. Therefore, the effects of UV damage in DNA (primarily by CPDs) must be local, and not propagate through an entire nucleosome length of DNA. If the 5S nucleosome were not able to accommodate UV photoproducts, we would expect to see either an alteration in the translational position or changes in the pattern of damage seen in the fraction of the reconstitutes that form nucleosomes versus the fraction that remains as free DNA. Regarding the latter case, however, we did not observe any differences for the major UV damage sites (Figure 4).

With regard to the primary position of the nucleosome on 5S rDNA, there has been some controversy as to the exact location of the dyad relative to the transcription start site. In an elegant study by Panetta et al. (*17*), the primary locations of nucleosomes were determined by a tethered hydroxyl radical footprinting technique. Although these authors used a longer fragment than ours (249 bp versus 214 bp), 42% of the nucleosomes had dyad positions of −3 or +7 (i.e., within one turn of the helix from the transcription start). The exact positions of the nucleosome dyad determined in our studies could not be as accurately determined as in Panetta et al. (*17*) due to some variation in the extent of micrococcal nuclease digestion (trimming the ends). Differences in the length and sequence upstream of the 5S rRNA gene may also account for the differences observed. For example, two of the major dyad positions found by Panetta et al. (*17*) would not permit a complete nucleosome core to form on our fragment. Most importantly for this study, however, is the fact that very little difference was observed between the UV-irradiated and unirradiated 5S rDNA fragments when digested side-by-side under identical conditions.

The effect of nucleosome folding on UV photoproduct formation was first reported over a decade ago (*10*). It was shown that the UV-induced photoproduct distribution in mixed sequence nucleosome core DNA is strongly modulated with an average periodicity of 10.3 bases. In addition, UV photoproduct formation is lowest in the central (∼30 bp) dyad axis region (*11*). Previously, it was reported that UV photoproduct formation in sea urchin 5S rDNA is not affected by nucleosome folding (*35*). This was deduced from the major effect of transcription factor binding, which overshadowed any effect due to nucleosome folding (*35*). Furthermore, the chemical cleavage method used in that study was not specific for CPDs and produced nonspecific cleavage of unirradiated DNA (*31*). However, in the present study, we have used the specific cleavage at CPDs by T4 endo V (*29*) to demonstrate a distinct inhibition of CPD formation in some sites of the nontranscribed strand of *Xenopus borealis* 5S rDNA (Figure 6). Most of these sites are within the dyad axis region of the 5S nucleosome (Figure 6), where the DNA may be underwound relative to the remainder of the core DNA helix (see below). Moreover, this region was shown to be the least susceptible to covalent binding by BPDE (*36*) and strand breaks induced by bleomycin and neocarzinostatin (*37*).

The inhibition of CPD formation reported here, as well as the inhibition observed for chemical adducts, can be explained by certain structural features of nucleosomal DNA. Hydroxyl radical footprinting yields a value of 10.2 bp/turn for the average helical periodicity of 5S rDNA in nucleosomes (*38*). Within the nucleosome core, however, this method yields a helical periodicity of 10.7 bp/turn for the central three turns of the 5S rDNA nucleosome and 10.0 bp/turn for the flanking regions (*16*). A similar change in helical periodicity is predicted by the UV photofootprint (i.e.,

modulated CPD pattern) observed for mixed sequence nucleosome cores (see introduction). These results predict that the central 30 bp of DNA (dyad region) are underwound relative to the standard B-form DNA structure (*39*). More recently, the crystal structure of the nucleosome core particle was reported at 2.8 Å resolution (*40*). The central three turns (or dyad region) are bound to the α-helices and protein main chain of the H3−H4 tetramer, and both the buried surface areas and number of protein−DNA contacts suggest the tightest binding within the nucleosome core occurs at ±0.5 turn from the dyad (*41*). Thus, since CPD formation requires rotation and bending of the DNA bases (*1*), our observation of a lower CPD yield in the central region (Figure 6) may reflect a decrease in DNA flexibility following nucleosome formation.

We also observed a correlation between CPD formation and rotational setting of a 14 nt pyrimidine tract of 5S rDNA in nucleosomes (Figure 7). As stated above, CPD formation in mixed sequence DNA is strongly affected by its rotational setting in nucleosomes with an average repeat of 10.3 bases (*10*). Furthermore, preexisting CPDs in DNA influence its rotational setting on the histone surface during nucleosome formation (*14*). More recently, it was found that the yields and distribution of CPDs in a defined-sequence nucleosome (HISAT) only partially resemble those of mixed-sequence nucleosomes (*15*). However, as observed for the pyrimidine tract in the 5S rDNA fragment (Figure 7), the sequence of HISAT DNA played a dominant role in the CPD distribution (*15*) and may have masked a subtle correlation with rotational setting.

It is likely that *both* sequence specificity *and* rotational setting are factors that determine CPD distribution in nucleosome DNA. In mixed sequence nucleosomes, the influence of rotational setting on CPD distribution is very apparent, since the probability of CPD formation is nearly the same at each site in the core DNA population (although see ref *42*). Therefore, a clear repeat pattern for CPD formation is seen in gel profiles (*10*). In the case of a unique sequence nucleosome, however, sequence specificity of CPD formation is most apparent, occurring only at dipyrimidine sites, and no simple 10 base repeat is obvious from the gel. However, as shown in Figure 7, a subtle correlation between CPD formation and rotational setting can be seen, once the dominant influence of sequence specificity is minimized by normalization. Thus, as with mixed sequence DNA, compression of the minor groove and reduced flexibility of DNA near the histone surface (*40*) plays a role in CPD formation in nucleosomes.

In conclusion, we found that (a) UV irradiation does not cause significant changes in the rotational and translational positioning of 5S rDNA in the nucleosome, (b) nucleosome folding modulates CPD formation in the dyad axis region of the nontranscribed strand of 5S rDNA where the DNA helix is tightly bound to the H3−H4 tetramer, and in addition to the strong sequence dependence, (c) the modulation of CPDs in a 14 nt pyrimidine tract of 5S rDNA correlates with its rotational setting in the nucleosome surface. These results help lay the foundation for the roles of specific structural features of nucleosomes in modulating UV photoproducts, as well as the effects of these photoproducts on nucleosome positioning.

ACKNOWLEDGMENT

We thank Dr. R. Stephen Lloyd for supplying purified T4 endonuclease V, and members of the Smerdon laboratory, as well as Dr. R. Reeves, Dr. F. Thoma, M. Nissen, and Dr. U. Schieferstein, for stimulating and critical discussions.

REFERENCES

1. Cadet, J., Anselmino, C., Douki, T., and Voituriez, L. (1992) *J. Photochem. Photobiol. B: Biol. 15*, 277−298.
2. Friedberg, E. C., Walker, G. C., and Siede, W. (1995) *DNA Repair and Mutagenesis*, American Society for Microbiology Press, Washington, DC.
3. Brash, D. E. (1988) *Photochem. Photobiol. 48*, 59−66.
4. Mullenders, L. H. F., Hazekamp-van Dokkum, A. M., Kalle, W. H. J., Vrieling, H., Zdzienicka, M. Z., and van Zeeland, A. A. (1993) *Mutat. Res. 299*, 271−276.
5. Wang, C. I., and Taylor, J. S. (1991) *Proc. Natl. Acad. Sci. U.S.A. 88*, 9072−9076.
6. Kim, J. K., Patel, D., and Choi, B. S. (1995) *Photochem. Photobiol. 62*, 44−50.
7. van Holde, K. E. (1989) *Chromatin*, Springer-Verlag, New York.
8. Wolffe, A. P. (1998) *Chromatin Structure and Function*, Academic Press, New York.
9. Smerdon, M. J., and Thoma, F. (1998) in *DNA Damage and Repair*, Vol. 2 (Nickoloff, J. A., and Hoekstra, M. F., Eds.) pp 199−222, Humana Press, Totowa, NJ.
10. Gale, J. M., Nissen, K. A., and Smerdon, M. J. (1987) *Proc. Natl. Acad. Sci. U.S.A. 84*, 6644−6648.
11. Gale, J. M., and Smerdon, M. J. (1988) *J. Mol. Biol. 204*, 949−958.
12. Brown, D. W., Libertini, L. J., Suquet, C., Small, E. W., and Smerdon, M. J. (1993) *Biochemistry 32*, 10527−10531.
13. Pehrson, J. R., and Cohen, L. H. (1992) *Nucleic Acids Res. 20*, 1321−1324.
14. Suquet, C., and Smerdon, M. J. (1993) *J. Biol. Chem. 268*, 23755−23757.
15. Schieferstein, U., and Thoma, F. (1996) *Biochemistry 35*, 7705−7714.
16. Hayes, J. J., Clark, D. J., and Wolffe, A. P. (1991) *Proc. Natl. Acad. Sci. U.S.A. 88*, 6829−6833.
17. Panetta, G., Buttinelli, M., Flaus, A., Richmond, T. J., and Rhodes, D. (1998) *J. Mol. Biol. 282*, 683−697.
18. Mann, D. B., Springer, D. L., and Smerdon, M. J. (1997) *Proc. Natl. Acad. Sci. U.S.A. 94*, 2215−2220.
19. Libertini, L. J., Ausio, J., van Holde, K. E., and Small, E. W. (1988) *Biophys. J. 53*, 477−487.
20. Lutter, L. C. (1989) *Methods Enzymol. 170*, 264−269.
21. Tullius, T. D., Dombroski, B. A., Churchill, M. E. A., and Kam, L. (1987) *Methods Enzymol. 155*, 537−558.
22. Meersseman, G., Pennings, S., and Bradbury, E. M. (1991) *J. Mol. Biol. 220*, 89−100.
23. Dong, F., Hansen, J. C., and van Holde, K. E. (1990) *Proc. Natl. Acad. Sci. U.S.A. 87*, 5724−5728.
24. Maniatis, T., Fritsch, E. F., and Sambrook, J. (1982) *Molecular Cloning: A Laboratory Manual*, Cold Spring Harbor Laboratory Press, Cold Spring Harbor, NY.
25. Li, S., Waters, R., and Smerdon, M. J. (2000) *Methods: A Companion to Methods in Enzymology* (in press).
26. Neubauer, B., and Horz, W. (1989) *Methods Enzymol. 170*, 630−644.
27. Huang, W. M., and Lehman, I. R. (1972) *J. Biol. Chem. 247*, 3139−3146.
28. Doetsch, P. W., Chan, G. L., and Haseltine, W. A. (1985) *Nucleic Acids Res. 13*, 3285−3304.
29. Dodson, M. L. and Lloyd, R. S. (1989) *Mutat. Res. 218*, 49−65.
30. Bohr, V. A., Smith, C. A., Okumoto, D. S., and Hanawalt, P. C. (1985) *Cell 40*, 359−369.
31. Becker, M. M., and Wang, Z. (1989) *J. Mol. Biol. 210*, 429−438.

32. Matsumoto, H., Takakusu, A., and Ohnishi, T. (1994) *Photochem. Photobiol. 60*, 134−138.
33. Matsumoto, H., Takakusu, A., Mori, T., Ihara, M., Todo, T., and Ohnishi, T. (1995) *Photochem. Photobiol. 61*, 459−462.
34. Reeves, R., and Wolffe, A. P. (1996) *Biochemistry 36*, 5063−5074.
35. Wang, Z., and Becker, M. M. (1988) *Proc. Natl. Acad. Sci. U.S.A. 85*, 654−658.
36. Thrall, B. D., Mann, D. B., Smerdon, M. J., and Springer, D. L. (1994) *Biochemistry 33*, 2210−2216.
37. Smith, B. L., Bauer, G. B., and Povirk, L. F. (1994) *J. Biol. Chem. 269*, 30587−30594.
38. Hayes, J. J., Tullius, T. D., andWolffe, A. P. (1990) *Proc. Natl. Acad. Sci. U.S.A. 87*, 7405−7409.
39. Pruss, D., Hayes, J. J., and Wolffe, A. P. (1995) *BioEssays 17*, 1−10.
40. Luger, K., Mader, A. W., Richmond, R. K., Sargent, D. F., and Richmond, T. J. (1997) *Nature 389*, 251−260.
41. Luger, K., and Richmond, T. J. (1998) *Curr. Opin. Struct. Biol. 8*, 33−40.
42. Jensen, K. A., and Smerdon, M. J. (1990) *Biochemistry 29*, 4773−4782.

BI991771M